Global risk mapping of highly pathogenic avian influenza H5N1 and H5Nx in the light of epidemic episodes occurring from 2020 onward

Marie-Cécile Dupas*[,1,2], Maria F. Vincenti-Gonzalez*[,1], Madhur Dhingra[3], Claire Guinat[4], Timothée Vergne[4], William Wint[5], Guy Hendrickx[6], Cedric Marsboom[1,6], Marius Gilbert[1], Simon Dellicour[1,7,8]

[1] Spatial Epidemiology Lab (SpELL), Université Libre de Bruxelles (ULB), Brussels, Belgium
[2] Data Science Institute, University of Hasselt
[3] Food and Agriculture Organization of the United Nations, Rome, Italy
[4] Interactions Hôtes-Agents Pathogènes (IHAP), Université de Toulouse, INRAE, ENVT, Toulouse, France
[5] Environmental Research Group Oxford Ltd, c/o Department of Biology, Mansfield Road, Oxford, OX1 3SZ
[6] Avia-GIS research department, Avia-GIS, Zoersel, Belgium
[7] Department of Microbiology, Immunology and Transplantation, Rega Institute, KU Leuven, Leuven, Belgium
[8] Interuniversity Institute of Bioinformatics in Brussels, Université Libre de Bruxelles, Vrije Universiteit Brussel, Brussels, Belgium
(*) denotes equal contribution

Abstract

Avian influenza (AI) is a highly contagious viral disease affecting poultry and wild water birds, posing significant global challenges due to its high mortality rates and economic impacts. Highly pathogenic avian influenza (HPAI) outbreaks, particularly those caused by H5N1 and its variants, have surged since their first occurrence in 1959. The HPAI H5N1 clade 2.3.4.4b viruses have notably expanded their geographical reach, affecting numerous countries, diverse avian species, and now wild and domestic mammals. Using an ecological niche modelling approach, this study aims to elucidate the environmental factors associated with the increased HPAI H5 cases since 2020, investigate potential shifts in ecological niches, and predict new areas suitable for local viral circulation. Focusing on H5N1 and H5Nx strains, we have developed ecological niche models for HPAI cases in both wild and domestic birds while considering two distinct periods: 2015-2020 and 2020-2022. Key environmental predictors include chicken and duck population density, human density, distance to water bodies, and several land cover variables. Post-2020, we observe a notable increase in the relative influence of some of these predictors, such as intensive chicken population density and cultivated vegetation. The resulting risk maps reveal notable ecological suitability for local HPAI H5 circulation in Europe, Asia, as well as North and South America, with notable expansions of the areas at risk post-2020. The spatial distribution of HPAI H5 occurrences in wild birds appears to be primarily correlated with urban areas and open water

regions. Overall, global risk maps derived from our models identify regions at risk where surveillance and control measures should be prioritised. Finally, our analyses also highlight a potential shift in the diversity of wild bird species affected by HPAI outbreaks, with a higher variety of avian species, particularly sea birds, being impacted post-2020. This increased diversity could suggest that ecological shifts in HPAI H5 circulation may be accompanied by a broader range of susceptible species. Overall, these results further contribute to the understanding of HPAI epidemiology.

Introduction

Since 2020, an increase in both H5Nx and H5N1 cases has been observed (Fig. 1). A variant of the Gs/Gd H5N1 viruses belonging to the H5 clade 2.3.4.4b has led to an unprecedented number of deaths in wild birds and poultry in many countries in Africa, Asia, and Europe (Huang et al., 2023). In 2021, the virus spread to North America, and in 2022, to Central and South America (FAO, WHO and WOAH, 2023) spilling over into poultry farms and infecting an alarming number of wild terrestrial, marine and domestic mammals (Elsmo et al., 2023; Leguia et al., 2023; Neumann and Kawaoka, 2024; Peacock et al., 2024; Plaza et al., 2024); marking an unprecedented expansion in the geography and impact of HPAI. In 2022, 67 countries across five continents reported H5N1 HPAI outbreaks in poultry and wild birds to the World Organisation for Animal Health (WOAH), resulting in over 131 million domestic poultry deaths or cullings (WOAH, 2023). In 2023, another 14 countries, mostly in the Americas, reported outbreaks. Several mass death events in wild birds were caused by influenza A(H5N1) clade 2.3.4.4b viruses (Klaassen and Wille, 2023; WOAH, 2023).

In that epidemiological context, understanding the environmental factors associated with the risk of HPAI circulation remains crucial. Extensive exploration of risk factors for HPAI presence, spread, and persistence has been conducted in various countries and regions. These studies have identified domestic waterfowl, several anthropogenic variables (human population density, distance to roads) and indicators of water presence as important factors for risk of H5N1 local circulation (Gilbert and Pfeiffer, 2012). More recent work on global suitability for HPAI have pinpointed that host-related variables such as poultry density are the strongest contributors to HPAI persistence (Dhingra et al., 2016; Gierak and Śmietanka, 2021; Martin et al., 2011).

In addition, poultry intensification, international poultry trade, live bird markets, and wild bird migratory routes have been recognised as playing a key role in the transmission and spread of HPAI (Vandegrift et al., 2010). Lastly, evidence of climate change impacting the dynamics of HPAI has also been discussed (Prosser et al., 2023). For example, changes in rainfall alter the distribution, abundance, and quality of wetlands can impact waterfowl populations (Forcey et al., 2007; Gilbert et al., 2008; Vandegrift et al., 2010). However, recent outbreaks raise questions about whether earlier ecological niche models still accurately predict the current distribution of areas ecologically suitable for the local circulation of HPAI H5 viruses. Ecological niche model outputs for range-shifting pathogens must therefore be interpreted with caution (Elith et al., 2010). Despite this limitation, correlative ecological niche models remain useful for identifying broad-scale associations and potential shifts in distribution. To account for this, we analysed two distinct time periods (2015-2020 and 2020-2023).

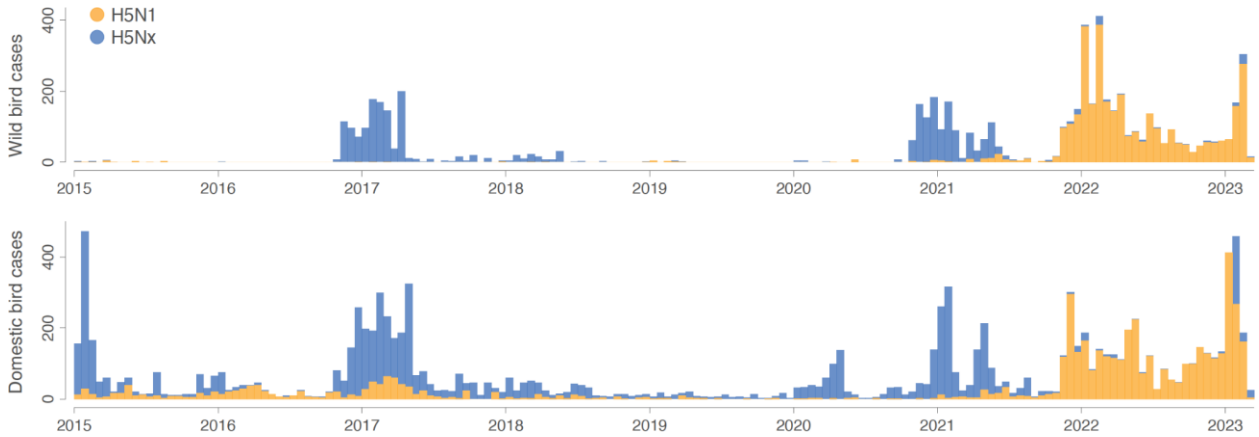

Figure 1: epidemic curves for both wild and domestic bird cases. Orange and blue histograms report the weekly number of H5N1 cases and the weekly number of H5Nx cases, respectively.

Understanding the interplay between environmental variables and avian influenza becomes increasingly crucial to have an in-depth understanding of the risk factors that govern avian influenza viruses (AIVs) circulation and spread. Following a previous study dedicated to the ecological niche of H5Nx and H5N1 (Dhingra et al., 2016), we aimed to address the following questions: (i) Which factors are associated with the increase in H5Nx and H5N1 cases since 2020? (ii) Do we observe a change or an extension of the ecological conditions suitable for local HPAI circulation? (iii) Are we able to predict the areas at risk for local HPAI circulation based on ecological niche models trained on occurrence data before 2020? To this end, we used HPAI H5N1 and H5Nx occurrence data collected before 2020 to train ecological niche models and tested whether these models could accurately predict areas ecologically suitable

for HPAI circulation post-2020. We developed separate ecological niche models for wild and domestic bird HPAI occurrences, as these two groups are influenced by different ecological processes, surveillance biases, and management contexts. These models thus predict the ecological suitability for the risk of local viral circulation leading to the detection of HPAI occurrences within each host group (rather than the niche of the virus or the host groups alone). Specifically, we employed a boosted regression trees (BRT) approach to estimate the HPAI ecological suitability given local environmental conditions. We also computed the diversity indices of wild bird species involved in HPAI occurrences, helping to understand how shifts in species diversity might correspond with the environmental factors considered in the ecological niche modelling analyses of HPAI in wild or domestic birds. Our results provide a better understanding of HPAI dynamics by identifying key environmental factors correlated with the increase in H5Nx and H5N1 cases in poultry and wild birds, investigating potential shifts in their ecological niches, and improving the prediction of at-risk areas. This knowledge might aid policymakers, epidemiologists, and wildlife conservationists in better targeting surveillance and control measures.

Results

In this study, we applied an ecological niche modelling approach using the boosted regression trees (BRT) method to evaluate the distribution of areas ecologically suitable for the risk of local circulation of HPAI H5Nx and H5N1 viruses in wild and domestic bird populations across two periods: 2015-2020 and 2020-2022. We trained separate ecological niche models for each combination of host groups (wild or domestic birds), virus strain (H5Nx or H5N1), and time period. In addition to evaluating each model separately, models trained on data from the 2015-2020 period were tested to predict occurrences in the 2020-2022 period, allowing us to evaluate the potential of pre-2020 models to predict a more recent distribution of H5N1 and H5Nx cases.

We assessed the relative influence (RI) of a broad range of spatial predictors (Elith et al., 2008), including anthropogenic, topographical, land cover, eco-climatic, and poultry density, on virus occurrences (Fig. S1). We used occurrence records from the EMPRES-i database and sampled pseudo-absence points to account for the lack of virus detection data in some areas. These pseudo-absence points were distributed based on human population density, with more pseudo-absence points sampled in areas of higher population to reflect the greater surveillance efforts in those regions (Fig. S2).

The accuracy of the models was validated through three types of cross-validation: (i) a standard cross-validation with a random and stratified divide between training and validation sets, (ii) a spatial cross-validation based on the approach used by Dhingra and colleagues (2016) that clustered presence and pseudo-absence points into folds using reference presence points, and (iii) a second spatial cross-validation based on a blocks generation technique (Valavi et al., 2019). Models using spatial cross-validation techniques are less affected by spatial autocorrelation, as shown by higher spatial sorting bias (SSB) values (Fig. S3). Among the seven datasets evaluated, four show better performance with the reference points-based spatial cross-validation method, suggesting it was less impacted by spatial autocorrelation compared to the block generation technique. Consequently, we have proceeded with the reference points approach for consistency with Dhingra et al. (2016).

Using pre-2020 data, our models demonstrated a relatively robust capability to predict the distribution of post-2020 occurrence data. The Area Under the Curve (AUC) values for ecological niche models trained on occurrence data in domestic birds before 2020 ranged between 0.74 and 0.77 when evaluated against post-2020 data, indicating a relatively good predictive performance. As expected, ecological niche models trained on post-2020 data showed a slightly higher predictive performance when evaluated on data from the same period, with AUC values ranging from 0.78 to 0.83 (Table S1). These results suggest that pre-2020 models captured broad patterns of suitability for H5Nx and H5N1 outbreaks, while post-2020 models provided a closer fit to the more recent epidemiological situation.

Previous literature reviews (Gilbert and Pfeiffer, 2012; Dhingra et al., 2016) have summarised the predictor variables commonly correlated with HPAI occurrences. As detailed in the Materials and Methods section and in the table in Supplementary Information Resources S1, we explored four sets of environmental variables considered by Dhingra and colleagues (Dhingra et al., 2016): host variables (set 1), land cover variables (set 2), eco-climatic variables (set 3), and a risk-based selection of variables performed by Dhingra and colleagues (set 4). Set 3 showed the lowest predictive performance for both domestic and wild bird cases during the two periods and, in contrast, sets 2 and 4 demonstrated the highest predictive accuracy for wild and domestic birds, respectively (Fig. S3). Set 4 combined host variables with cultivated and managed vegetation, open water areas, distance to water, and the annual mean of land surface temperature. For domestic birds, set 1 (host variables) performed well before 2020, but its predictive

performance decreased after 2020 in favour of set 4. Ecological niche models trained on wild and domestic bird cases, respectively with the sets 2 and 4, are associated with AUC values exceeding 0.77, indicating a relatively strong performance in predicting H5 occurrences based on these sets of environmental variables.

Figure 2 displays the response curves of the most important variables with their respective RI (Table S2). In the ecological niche models for H5N1 and H5Nx in domestic birds, the densities of intensive chicken populations, domestic duck populations, and human populations emerged as significant predictors, each with RI values exceeding 5%. Notably, the RI for intensive chicken density in H5N1 models increased sharply from 8.5% to 30.4% since 2020. Similarly, the RI of cultivated and managed vegetation has doubled for both strains post-2020. The response curves showed a positive correlation, indicating that higher values of these predictors were linked with an increased likelihood of HPAI occurrences given local environmental conditions. These findings indicate a trend towards increased HPAI susceptibility in environments characterised by intensive agricultural and vegetation management practices.

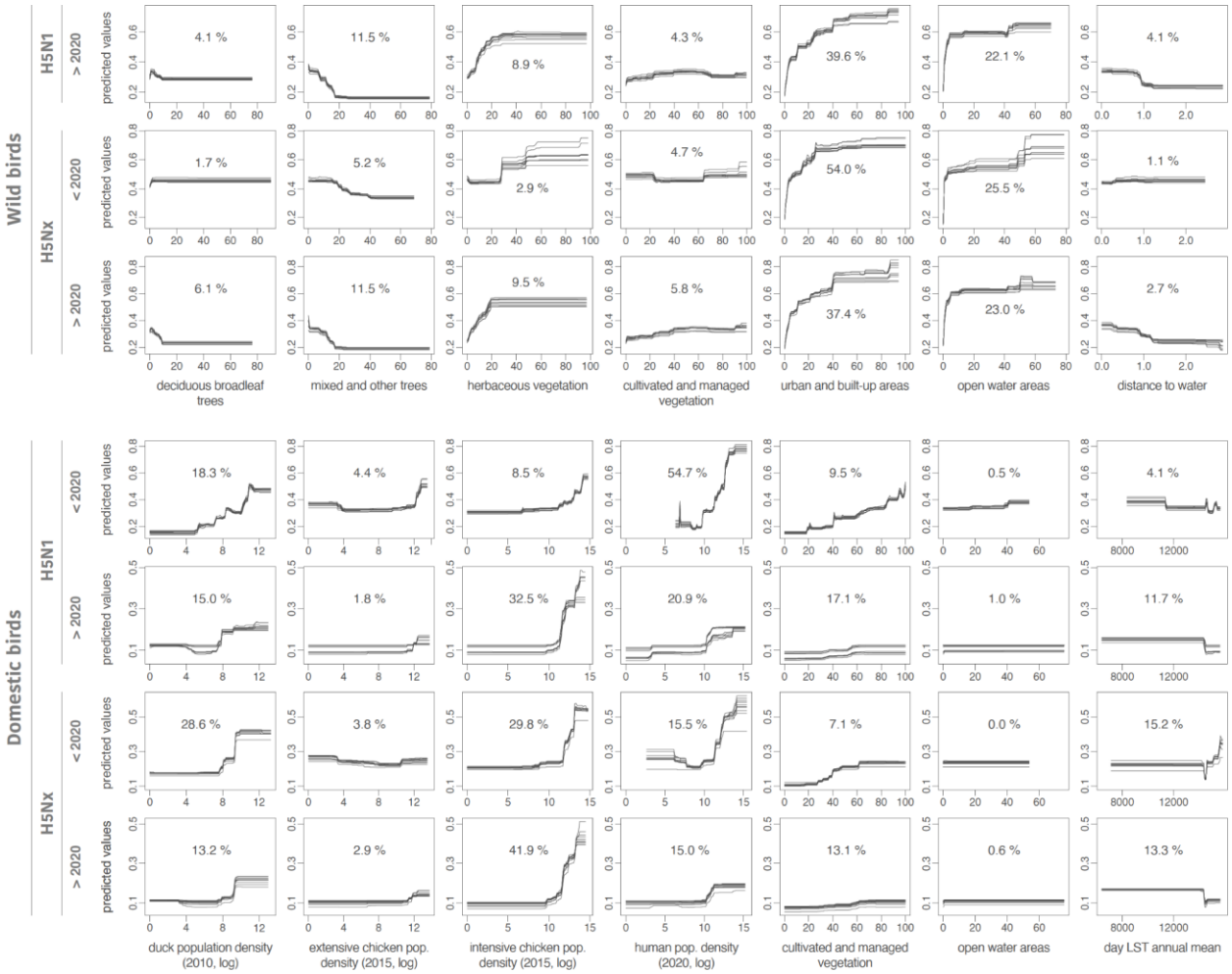

Figure 2: response curves associated with the environmental variables included in the ecological niche models. For the ecological niche models trained on wild bird infection records, we here only display the response curves estimated for the environmental variables associated with an averaged relative influence (RI) >4% for at least one of the considered occurrence datasets (thus not reporting the response curves obtained for the following variables: evergreen deciduous needleleaf trees, evergreen broadleaf trees, shrublands, and regularly flooded vegetation). Each curve was retrieved from a distinct boosted regression tree (BRT) model trained for a specific dataset of occurrence data. We also report the averaged RI (in %) of each environmental variable in the respective ecological models trained on a specific dataset of occurrence data (see Table S1 for the complete list of RI estimates along with their first and third quartiles). Due to lack of data, the model was not trained for H5N1 in wild birds before 2020.

In contrast, eco-climatic factors such as land surface temperature and precipitation (set 3) showed only moderate influence. We also observed a decrease in the importance of domestic duck population density for both subtypes after 2020, possibly due to the increasing diversity of bird species involved in the transmission dynamics of H5N1 and H5NX (Fig. S4). These findings highlight the crucial role of anthropogenic and host-related variables in accurately predicting HPAI occurrences.

168

169 In the ecological niche models trained for wild bird cases, urban and built-up areas were associated with H5N1 and
170 H5Nx occurrences (Fig. 2), showing the highest relative influence (RI) prior to 2020. Specifically, RI values reached
171 54.5% before 2020 but decreased to 39.3% in the post-2020 period. This decline may indicate a reduced bias in
172 observation data: typically, dead wild birds are more frequently found near human-populated areas due to
173 opportunistic detections, whereas more recent surveillance efforts have become increasingly proactive (Giacinti et
174 al., 2024). After 2020, we observed an increase in the importance of habitats, such as deciduous broadleaf trees
175 (6.1%), mixed and other tree regions (11.4%), and herbaceous vegetation for H5Nx (9.5%). However, response curves
176 (Fig. 2) indicated that H5N1 and H5Nx occurrences in wild birds decreased in areas with greater tree cover, while it
177 increased in regions dominated by herbaceous vegetation. Open water areas consistently showed high RI values
178 across all time periods and virus strains, particularly for H5Nx before 2020 (25.5%) and H5N1 after 2020 (22.0%),
179 highlighting their significant role in the ecological models of HPAI outbreaks.

180

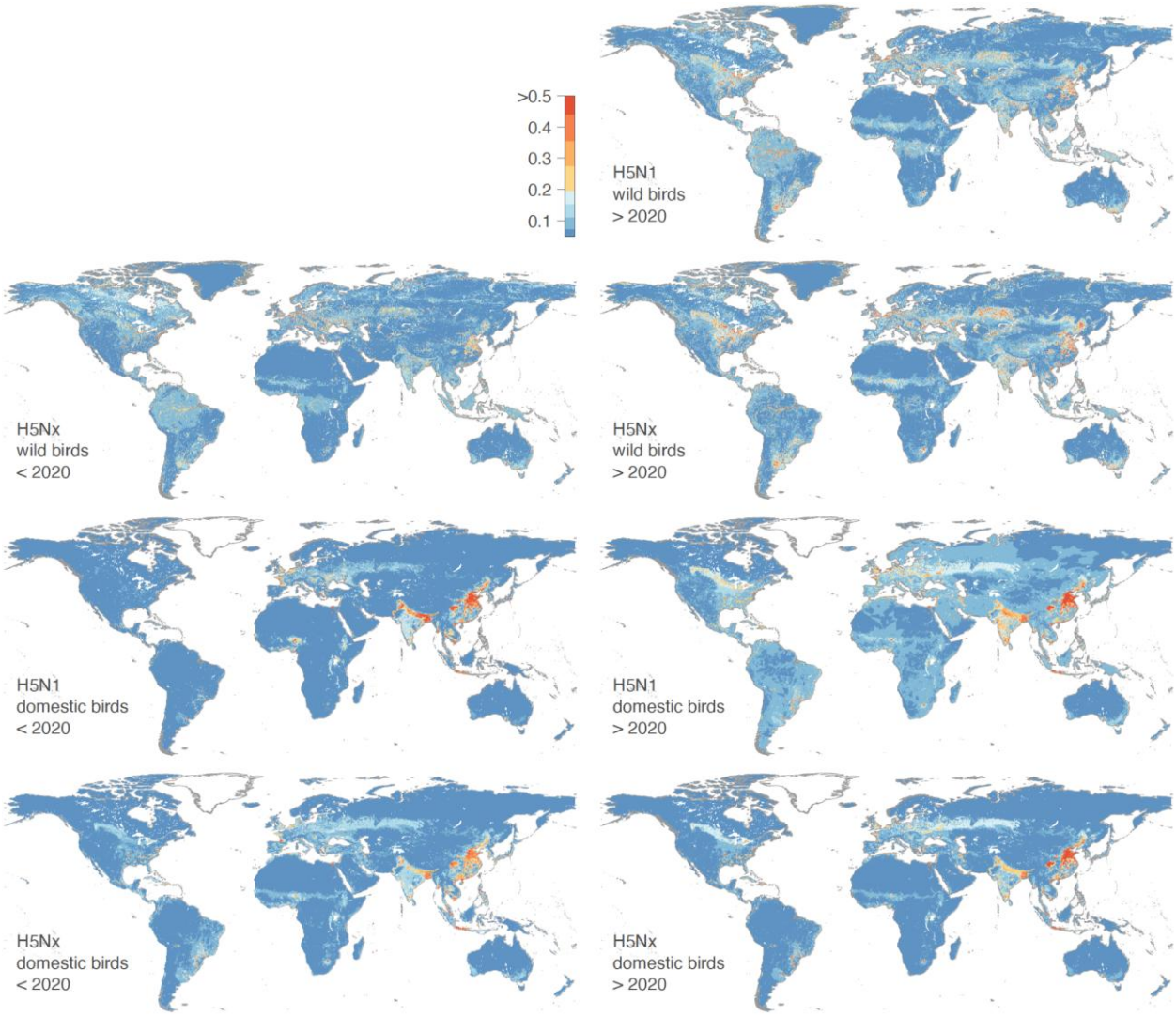

Figure 3: areas ecologically suitable for local H5N1 or H5Nx circulation leading to infection cases in domestic bird populations. We estimated the ecological suitability for two different time periods (2015-2020 and 2020-2022) and for both wild and domestic bird populations. Dynamic visualisations of the results are available here: https://mood-platform.avia-gis.com/core.

Figure 3 displays maps of the predicted ecological suitability for the risk of local H5N1 and H5NX circulation across two time periods, 2015-2020 and 2020-2022; these maps being also accessible on the following link for a dynamic visualisation of the results: https://app.mood-h2020.eu/core. All maps are in a WGS84 projection with a spatial resolution of 0.0833 decimal degrees (i.e. 5 arcmin, or approximately 10 km at the equator). For H5N1 and H5Nx in domestic birds, these maps reveal several regions associated with a relatively high ecological suitability, especially in Europe and Asia, in countries such as South Korea, Japan, Singapore, Malaysia, Vietnam, Cambodia, Thailand, and the Philippines, as well as the United Kingdom, France, the Netherlands, Germany, Italy, Ukraine, and Poland. Additionally, several areas in African nations, including Nigeria and South Africa, were identified as suitable

environments for both H5N1 and H5Nx local circulation in scenarios before and after 2020. Regions in North America and South America — including Bolivia, Brazil, Colombia, Ecuador, Chile, Peru, and Venezuela — demonstrated ecological suitability for the risk of local circulation for H5Nx and H5N1, with a marked increase in the predicted suitability for H5N1 after 2020. For H5Nx post-2020, areas of high predicted ecological suitability, such as Brazil, Bolivia, the Caribbean islands, and Jilin province in China, likely result from spatial extrapolations, as these regions reported few or no outbreaks in the training data.

Our findings were overall consistent with those previously reported by Dhingra and colleagues (Dhingra et al., 2016), who used data from January 2004 to March 2015 for domestic poultry. However, some differences were noted: their maps identified higher ecological suitability for H5 occurrences before 2016 in North America, West Africa, eastern Europe, and Bangladesh, while our maps mainly highlight ecologically suitable regions in China, South-East Asia, and Europe (Fig. S5). In India, analyses consistently identified high ecologically suitable areas for the risk of local H5Nx and H5N1 circulation for the three time periods (pre-2016, 2016-2020, and post-2020). Similar to the results reported by Dhingra and colleagues, we observed an increase in the ecological suitability estimated for H5N1 occurrence in South America's domestic bird populations post-2020. Finally, Dhingra and colleagues identified high suitability areas for H5Nx occurrence in North America, which are predicted to be associated with a low ecological suitability in the 2016-2020 models.

For H5Nx and H5N1 cases in wild birds, the estimated ecological niches were primarily associated with environmental factors such as open water and distance to water, which result in ecological suitability hotspots estimated near coasts and main rivers. For both H5Nx and H5N1, certain areas of predicted high ecological suitability appear spatially isolated, i.e. surrounded by regions of low predicted ecological suitability. These areas likely meet the environmental conditions associated with past HPAI occurrences, but their spatial isolation may imply a lower risk of actual occurrences, particularly in the absence of nearby outbreaks or relevant wild bird movements. Some of the areas with high predicted ecological suitability reflect the result of extrapolations. This is particularly the case in coastal regions of West and North Africa, the Nile Basin, Central Asia (Kyrgyzstan, Tajikistan, Uzbekistan), Brazil (including the Amazon and coastal areas), southern Australia, and the Caribbean, where ecological conditions are similar to those in areas where outbreaks are known to occur but where records of outbreaks are still rare.

We observed that areas of relatively high ecological suitability have expanded after 2020. North America, particularly near the Great Lakes region, appeared more suitable for local H5Nx circulation. This expansion was also evident in Russia and South America, aligning with major bird migration routes. Notably, while H5Nx had not been reported in Australia, the models indicate potential ecological suitability there as well. Expanded ecological suitability was also observed in China, India, and European countries. However, models trained on pre-2020 data maintained reasonable predictive performance when tested on post-2020 data, suggesting that the overall ecological niche of HPAI did not drastically shift over time.

In Table 1, we report the estimation of avian species diversity indices for species involved in HPAI outbreaks for the pre-2020 and post-2020 periods. Note that these indices reflect the diversity of bird species detected in outbreak records, not necessarily their abundance in the wild. We observed variations between these two periods both in the overall bird population and within specific wild bird species groups, including sea bird species (e.g., gulls, terns, boobies, gannets). For all birds, the Shannon index increased from 4.23 before 2020 to 5.03 after 2020, which might indicate a more diverse infected bird population in the latter period. The Simpson index however only rose from 0.97 to 0.98, but which could potentially suggest a slightly higher concentration of certain species post-2020. Sea birds exhibited a similar upward trend in diversity post-2020, with the Shannon index increasing from 2.19 to 2.26. This latter trend could potentially suggest a broader diversity of sea bird species involved in HPAI outbreaks.

When considering wild birds affected by the H5N1 strain of HPAI, there is a notable increase in the Shannon index from 2.00 before 2020 to 2.95 after 2020, accompanied by a rise in the Simpson index from 0.83 to 0.91. These increases could be indicative of greater diversity and a more even distribution of wild bird species among the reported HPAI H5N1 wild bird cases after 2020. In contrast, birds not affected by the H5N1 strain showed a slight decrease in diversity post-2020. The Shannon index decreases from 3.42 to 3.26, and the Simpson index decreases from 0.95 to 0.92. Given that HPAI particularly affected sea birds >2020, we further explore the yearly distribution of sea bird families. As depicted in Figure S4, positive cases among sea birds belonging to the families Laridae (gulls and terns), Sulidae (gannets and boobies), Ardeidae (herons), Pelecanidae (pelicans), Spheniscidae (penguins), Alcidae (auks), Phalacrocoracidae (cormorants) were detected more frequently from 2020 in comparison to before

2020. Notably, the occurrence of Laridae and Sulidae species among positive cases increased markedly from 2021 onwards.

Table 1. Species diversity indices estimated from infected bird cases before and after 2020. This table presents the Shannon and Simpson species diversity indices for various bird groups, comparing values before and after the year 2020. The indices are provided for all birds, sea birds, wild birds, domestic birds, as well as all birds affected by H5N1 and non-H5N1 strains.

	All birds		**Sea birds**		**Wild birds**		**Domestic birds**		**All birds H5N1**		**All birds non-H5N1**	
	Shannon	*Simpson*	*Shannon*	*Simpson*	*Shannon*	*Simpson*	*Shannon*	*Simpson*	*Shannon*	*Simpson*	*Shannon*	*Simpson*
< 2020	4.227	0.971	2.187	0.843	3.072	0.832	3.919	0.966	2.003	0.833	3.415	0.945
> 2020	5.033	0.982	2.255	0.831	5.066	0.983	2.967	0.897	2.952	0.907	3.254	0.914

To evaluate whether the post-2020 increase in species diversity estimated for infected wild birds could result from an increase in the number of tests performed on wild birds, we compared European annual surveillance test counts (EFSA et al., 2025, 2019) before and after 2020 using a Wilcoxon rank-sum test. We relied on European data because it was readily accessible and offered standardised and systematically collected metrics across multiple years, making it suitable for a comparative analysis. Although borderline significant (p-value = 0.063), the Wilcoxon rank-sum test indeed highlighted a recent increase in the number of wild bird tests (on average >11,000/year pre-2020 and >22,000 post-2020), which indicates that the comparison of bird species diversity metrics should be interpreted with caution. However, such an increase in the number of tests conducted in the context of a passive surveillance framework would thus also be in line with an increase in the number of wild birds found dead and thus tested. Therefore, while the increase in the number of tests could indeed impact species diversity metrics such as the Shannon index, it can also reflect an absolute higher wild bird mortality in line with a broadened range of infected bird species.

Discussion

Using an ecological niche modelling approach, our study presents an analysis of the ecological suitability, interpreted here as the risk of local circulation, for H5Nx and H5N1 HPAI viruses across different temporal and ecological contexts. By conducting boosted regression tree (BRT) analyses and incorporating a diverse set of spatial predictors, our study provides insights into the environmental and anthropogenic factors that are correlated with the distribution of these viruses in both wild and domestic bird populations. For domestic birds, our results concur with those previously reported by Dhingra and colleagues (Dhingra et al., 2016), indicating that ecological niche models

incorporating host variables (chicken and duck population densities) outperform those based on land-use or eco-climatic factors in terms of predictive performance. Contrariwise, in our analysis of H5N1 and H5Nx HPAI in wild birds, the most significant predictors were anthropogenic factors, notably urban areas and distance to open water. However, observation biases might affect these findings since outbreaks in wild birds are commonly reported near human populations.

In our analyses, intensive chicken population density emerges as a significant predictor, underscoring the strong association of poultry farming practices with HPAI spread (Dhingra et al., 2016) and revealing a complex interplay between ecological niches and the anthropogenic landscape. We note, however, that intensive poultry density may reflect both surveillance intensity and epidemiological risk, and its predictive role in our models should be interpreted in light of both processes. Similarly to the results of Dhingra and colleagues (Dhingra et al., 2016), land-use and climatic predictors do not play an important role in the niche ecological models, even for wild birds. This suggests that HPAI H5Nx is not as strongly environmentally constrained as vector-borne pathogens, for which clear eco-climatic boundaries (e.g., vector borne diseases) can be mapped (Dhingra et al., 2016). Additionally, we found that while domestic duck population density is a significant predictor for HPAI occurrence in domestic birds before 2020, its importance has decreased post-2020, particularly within the H5Nx ecological niche model. This observation is particularly noteworthy, as domestic ducks have historically been closely linked to areas of persistence and evolution of H5N1 HPAI (Gilbert and Pfeiffer, 2012). However, our findings, in line with earlier studies such as the one of Dhingra and colleagues (Dhingra et al., 2016), highlight a significant shift in the epidemiological dynamics of HPAI. Specifically, while the association between the H5Nx clade 2.3.4.4 and domestic ducks has for instance been documented in South Korea (Hill et al., 2015), it is becoming increasingly evident that HPAI is now more strongly associated with high-density chicken farming and anthropogenic factors. This shift suggests that the virus could now be circulating more among farms (farm to farm transmission) (FAO, 2023), with fewer introductions by wild birds — particularly wild ducks, which have previously acted as "Trojan horses" for H5N1 HPAI (Kim et al., 2014). However, this remains an interpretation, as the available data do not allow us to distinguish between index cases and secondary transmission events. Consequently, we could be witnessing a shift from the traditional duck/rice ecosystems towards a scenario where intensive chicken farming and a wider diversity of wild birds play a more prominent role in the transmission dynamics of HPAI. Therefore, monitoring areas with high intensive chicken

densities and regular surveillance of wild birds remain crucial for the early detection and management of HPAI outbreaks.

A difference between the ecological niche models previously trained by Dhingra and colleagues (Dhingra et al., 2016) and our models is the pronounced increase in ecological suitability for H5N1 in domestic bird populations estimated in India and China. More generally, our models highlight the extensive spread of H5N1 and H5Nx HPAI among domestic birds in Asia previously identified as “reassortment sink areas” (Dhingra et al., 2018). Reassortment refers to the process where influenza viruses exchange genetic material, potentially leading to new, more virulent strains. The extent of virus suitability in Asia highlights a potential change in the dynamics of virus spread, possibly driven by intensified poultry farming practices and increased human-wildlife interactions in these regions (Bahl et al., 2016; Gilbert et al., 2017).

The recent outbreaks of infection in cattle within the United States have been partially delineated by our HPAI risk mapping approach, highlighting major hotspots predominantly in the Great Lakes region, including Michigan. From March to July 2024, approximately 26 herds in Michigan were affected (U.S. Department of Agriculture, 2024). Additionally, our risk maps identify localised hotspots around urban centres in Colorado and Texas, where herds have also been infected. These outbreaks appear to stem from a single introduction event in Texas by wild birds (Worobey et al., 2024a, 2024b). This trend may be indicative of an increasing risk of future introductions from wild birds, as we observed a significant rise in the diversity of infected bird species after 2020, particularly among sea birds.

The latest strain of H5N1 (H5 clade 2.3.4.4b), believed to have emerged in 2014, shows adaptations for infecting a wide range of wild birds and mammals (Caliendo et al., 2022; Graziosi et al., 2024). By 2020, its spread among wild birds was three times faster than in farmed poultry due to mutations enabling the virus to infect diverse species (CDC, 2024; Xie et al., 2023). Unlike previous epidemic waves in Europe, outbreaks in the last years have also continued through summer, confirming that the virus's current circulation is no longer seasonal but nesting in the wild bird population (Sciensano, 2024). Therefore, the virus is able to infect a wider range of species than previous forms, as it circulates all seasons (Sacristán et al., 2024). The densely packed colonies of sea birds have also facilitated

the rapid virus spread, resulting in high mortality in these sea bird colonies (Boulinier, 2023; Bregnballe et al., 2024). For instance, the Netherlands lost up to 80% of its Sandwich terns in weeks, and the UK saw significant outbreaks, especially on Scottish islands (Knief et al., 2024). In South America, similar trends have been observed, with notable die-offs in seabird populations along coastal regions, particularly impacting species such as penguins, pelicans and cormorants (Leguia et al., 2023). Since then, in early 2023, the Peruvian outbreak had spread to marine mammals, particularly affecting the South American sea lion, which also began to experience a mass die-off (Campagna et al., 2024; Leguia et al., 2023).

The increase in the number of wild bird species being infected by HPAI, particularly H5N1, could be attributed to several factors such as viral evolution, increased interaction between domestic and wild birds, climate and land-use changes, among others. Regarding land-use changes, large parts of Europe have become increasingly fragmented due to the expansion of urban and transport infrastructure (European Environment Agency (EEA), 2022). This habitat loss and fragmentation can significantly impact water availability and trophic resources (Santos-Tovar et al., 2024), which could in turn aid the spread and transmission of avian influenza viruses due to relocation of birds and outbreaks (Yin et al., 2022). Climate change has also been reported as a factor that could affect wild bird distribution in different ways (Gilbert et al., 2008). As global climate conditions change, avian migratory patterns and routes are also changing (Hitch and Leberg, 2007; Van Doren, 2022). Furthermore, higher temperatures and extreme weather have resulted in large-scale population shifts in a range of temperate species (Dezfuli et al., 2022). Overall, these elements therefore raise the question of the role of climate and land-use changes in the recent shifting epidemiology of HPAI in wild birds.

The increasing diversity of infected bird species is part of a broader resurgence of H5N1 globally. Phylogenetic analysis from Europe revealed significant genetic diversity in HPAI-H5N1 viruses since October 2020, likely due to multiple reassortment events with LPAI viruses. Notable introductions from Russia to Europe were observed through autumn migrations of wild birds (ECDC, 2021). Additionally, the transatlantic transport of HPAI H5N1, documented in Canada in December 2021, suggests the virus can spread across continents, a route previously seen only with LPAI viruses (Caliendo et al., 2022; Dusek et al., 2014; Huang et al., 2014). In November 2022, H5N1 (clade 2.3.4.4b) was introduced into South America, presumably through the movements of migratory wild birds travelling south during

360 the boreal winter. The virus spread rapidly and caused significant mortality in wild birds and marine mammals across
361 multiple countries (Leguia et al., 2023; (Banyard et al., 2023; Campagna et al., 2024; Gamarra-Toledo et al., 2023;
362 WOAH, 2024).
363
364 Interestingly, our models spatially extrapolate ecological suitability for H5Nx in wild birds in areas where few or no
365 outbreaks have been reported. This discrepancy may be explained by limited surveillance or underreporting in those
366 regions. For instance, there is significant evidence that Kazakhstan and Central Asia play a role as a centre for the
367 transmission of avian influenza viruses through migratory birds (Amirgazin et al., 2022; FAO, 2005; Sultankulova et
368 al., 2024). However, very few wild bird cases are reported in EMPRES-i. In contrast, Australia appears
369 environmentally suitable in our models, yet no incursion of HPAI H5N1 2.3.4.4b has occurred despite the arrival of
370 millions of migratory shorebirds and seabirds from Asia and North America. Extensive surveillance in 2022 and 2023
371 found no active infections nor evidence of prior exposure to the 2.3.4.4b lineage (Wille et al., 2024; Wille and
372 Klaassen, 2023).
373
374 Despite the robustness of our ecological niche models, some limitations must be acknowledged. Firstly, the accuracy
375 of our models is inherently dependent on the quality and completeness of the occurrence data used, which is
376 influenced by the different reporting systems in place in different countries. Secondly, the definitions of key
377 explanatory variables, such as intensive versus extensive production, may vary across regions, adding complexity to
378 global predictions. To address these limitations, future work could focus on developing country-level or regional
379 models that incorporate localised data and context-specific definitions. Thirdly, underreporting and biases in
380 outbreak reports, particularly in wild bird populations, can skew model predictions and underestimate areas at risk.
381 Furthermore, another limitation of our models for wild bird populations is the lack of incorporation of migratory
382 patterns and behaviours. Migratory birds have complex movement patterns influenced by seasonal changes, food
383 availability, and habitat conditions. Our models, using static spatial predictors, do not capture these dynamic routes
384 and stopover sites, leading to potential inaccuracies in predicting areas at risk for HPAI circulation. In future work,
385 the integration of dynamic migratory data and environmental changes into our ecological niche models could
386 provide a more comprehensive and accurate risk assessment for HPAI spread among wild bird populations. In
387 addition, aligning outbreak occurrences with seasonally matched environmental variables could further refine

388 predictions of HPAI risk linked to migratory dynamics. Finally, our models for domestic poultry do not distinguish
389 between primary introduction events (e.g., spillover from wild birds) and secondary transmission between farms
390 due to limitations in the available surveillance data. While environmental factors likely influence the risk of initial
391 spillover events, secondary spread is more often driven by anthropogenic factors such as biosecurity practices and
392 poultry trade, which are not included in our current modelling framework.
393
394 Despite these limitations, our study provides significant contributions to the understanding of H5N1 and H5Nx HPAI
395 virus dynamics. By integrating a wide range of spatial predictors and using ecological niche modelling techniques,
396 we provide a quantitative analysis on the factors driving virus distribution. Overall, our study underscores the
397 importance of continuous surveillance and the need for adaptive management strategies to address the evolving
398 threat of HPAI viruses globally.
399

400 Materials and Methods

401 Our approach is similar to the one implemented by Dhingra and colleagues (2016). While Dhingra et al. (2016)
402 developed their models only for domestic birds over the 2003-2016 period, our models were developed for two host
403 groups separately (wild and domestic birds) and for two time periods (2016-2020 and 2020-2023).
404

405 *HPAI occurrence data acquisition*

406 The dataset containing highly pathogenic avian influenza (HPAI) occurrences was constructed by extracting relevant
407 information from the EMPRES-i database spanning the period from January 5, 2015, to March 7, 2023. This dataset
408 encompasses comprehensive details pertaining to H5N1 and H5Nx subtypes, including the family of birds involved
409 in transmission, observation and reporting dates, location coordinates, and the respective countries where the
410 reports originated. The dataset comprises a total of 17,410 H5Nx and 8,383 H5N1 reported cases. It is important to
411 note that the EMPRES-i database does not distinguish between index cases (e.g., primary spillover from wild birds)
412 and secondary farm-to-farm transmissions. As such, our ecological niche models are trained on confirmed HPAI
413 outbreaks in poultry that may result from different transmission dynamics — including both initial introduction
414 events influenced by environmental factors and subsequent spread within poultry systems.

Environmental data acquisition

Previous literature reviews (Gilbert and Pfeiffer, 2012; Dhingra et al., 2016) have summarised the predictor variables commonly linked to occurrences of HPAI. Here, we explored four sets of environmental variables considered by Dhingra and colleagues (Dhingra et al., 2016), and which are detailed in the table in Supplementary Information Resources S1: host variables (set 1), land cover variables (set 2), eco-climatic variables (set 3), and a risk-based selection of variables performed by Dhingra and colleagues (set 4).

Set 1 includes $\log_{10}$-transformed extensive and intensive chicken density (Gilbert et al., 2015), domestic duck density (Robinson et al., 2014) and human population density from the Gridded Population of the World (Center For International Earth Science Information Network-CIESIN-Columbia University, 2017) database. The chicken density data includes GIS layers representing the global distribution of chickens, categorised into extensive and intensive systems. It uses the model published by Gilbert et al. (2018) applied to the Gridded Livestock of the World (GLW) version 3 chicken layers (Gilbert et al., 2022a). The global domestic duck distribution data were computed using the GLW version 4 (Gilbert et al., 2022b). Set 2 includes land cover information, which was obtained from the global 1-km Consensus Land Cover database by (Tuanmu and Jetz, 2014) Tuanmu and Jetz (2014), and identifies different land cover categories by providing a percentage of representation of each land cover category within raster cells of approximately one square kilometre (http://www.earthenv.org/landcover.html). Additionally, this dataset was supplemented by a layer about the distance of each spatial point to the open water. Set 3 encompasses seasonal and large-scale patterns of eco-climatic indices like daytime land surface temperature (day LST) and the normalised difference vegetation index (NDVI), as documented by Scharlemann and colleagues (Scharlemann et al., 2008). Finally, set 4 is a selection from the previous sets based on prior epidemiological knowledge (Gilbert and Pfeiffer, 2012; Dhingra et al., 2016).

Ecological niche modelling

The different ecological niche modelling analyses were performed with the boosted regression trees (BRT), available in the R package “dismo” (Hijmans et al., 2017). BRT is a machine learning approach that can be used to generate a collection of sequentially fitted regression trees optimising the predictive probability of occurrence given local

environmental conditions (Elith et al., 2006). The predictive probability, interpreted as ecological suitability for local virus circulation, ranges from “0” (unsuitable environmental conditions) and “1” (highly suitable environmental conditions). BRT allows us to model complex non-linear relationships between the response and various predictor variables (Elith et al., 2008). It has also been demonstrated that the BRT approach had a superior predictive performance compared to alternative modelling approaches (Elith et al., 2006).

We selected 2020 as a cut-off point to reflect a well-documented shift in HPAI epidemiology, notably the emergence and global spread of clade 2.3.4.4b. This event marked a turning point in viral dynamics, influencing both the range of susceptible hosts and the geographical distribution of outbreaks. Based on this distinction, we performed ten replicated BRT analyses using each of the seven occurrence datasets: (i) H5Nx cases in wild birds < 2020 (01/01/2015 - 31/12/2019), (ii) H5N1 cases in wild birds > 2020 (01/01/2020 - 06/03/2023), (iii) H5Nx cases in wild birds > 2020 (01/01/2020 - 06/03/2023), (iv) H5Nx cases in domestic birds < 2020 (01/01/2015 - 31/12/2019), (v) H5N1 cases in domestic birds < 2020 (01/01/2015 - 31/12/2019), (vi) H5N1 cases in domestic birds > 2020 (01/01/2020 - 06/03/2023), and (vii) H5Nx cases in domestic birds > 2020 (01/01/2020 - 06/03/2023). Of note, there was not enough occurrence data to train ecological niche models on H5N1 cases in wild birds < 2020 (only 33 occurrence data from eight different countries — Bangladesh, Bulgaria, China, India, Kazakhstan, Nepal, Romania, and Russia — between the 01/01/2015 and 31/12/2019).

We ran BRT analyses using both occurrence and “pseudo-absence” data, the latter corresponding to randomly sampled absence points within the study area (Elith et al., 2006). To account for heterogeneity in AIV surveillance and minimise the risk of sampling pseudo-absences in poorly monitored regions, we restricted our analysis to countries (or administrative level 1 units in China and Russia) with at least five confirmed outbreaks. Unlike Dhingra et al. (2016), who sampled pseudo-absences across a broader global extent, our sampling was limited to regions with demonstrated surveillance activity. In addition, we adjusted the density of pseudo-absence points according to the number of reported outbreaks in each country or admin-1 unit, as a proxy for surveillance effort — an approach not implemented in this previous study.

470 In addition, the sampling pseudo-absence points was based on the human population distribution to further account
471 for potential within country differences in surveillance intensity (Dhingra et al., 2016): the probability to sample a
472 pseudo-absence from a given grid cell was proportional to the log-transformed human population density in that
473 cell. The human population density raster was retrieved from the Gridded Population of the World (GPW) project,
474 which was downscaled to a resolution of 5 arcminutes. Another approach to sampling pseudo-absences would have
475 been to distribute them according to the density of domestic poultry. However, as pointed out by Dhingra and
476 colleagues (2016), the locations of outbreaks in the EMPRES-i database are often georeferenced using place name
477 nomenclatures due to a lack of accurate GPS data, which could introduce a spatial bias towards populated areas.
478 Therefore, the use of human population density as an indicator of surveillance effort takes into account not only the
479 probability of detection, but also the geo-referencing bias in household records. To further reduce bias from
480 unsuitable regions where the pathogen may not have been introduced, we restricted pseudo-absence sampling to
481 areas located at a minimum of 10 km and a maximum of 1,000 km from known presence points (Phillips et al., 2009;
482 Dhingra et al., 2016). Initially, ten times more pseudo-absences than presence points were simulated, but we
483 ultimately retained three times more pseudo-absences than presences in each country/admin-1 unit.
484
485 Given that spatial data typically exhibits autocorrelation, employing a standard cross-validation procedure may
486 result in an overestimation of the BRT model's accuracy (Randin et al., 2006). To circumvent this issue, we employed
487 a spatial cross-validation procedure to select the optimal number of trees in each BRT model. Specifically, we tested
488 and compared two distinct spatial cross-validation procedures: (i) the procedure introduced by Dhingra and
489 colleagues and based on (five) reference presence points used to cluster the presence and pseudo-absence points
490 in (five) folds according to their nearest distance to a reference point, and (ii) the procedure introduced by Valavi
491 and colleagues and based on a block generation method (Valavi et al., 2019). In the first spatial cross-validation
492 procedure, the five reference presence points were randomly selected among all presence points. If each of the five
493 generated spatial folds did not gather at least 10% of the presence points, the random selection of reference points
494 was re-initiated. To compare the performance of the three cross-validation procedures applied in this study (the
495 standard procedure and the spatial procedures based on the reference points or blocks generation), we estimated
496 the spatial sorting bias (SSB) metric (Hijmans, 2012) ranging from 0 to 1, an SSB near 0 and 1 indicating an extreme
497 impact and the absence of an impact of spatial autocorrelation on the model training, respectively.

All BRT analyses were run and averaged over 10 cross-validated replicates, with a tree complexity of 4, a learning rate of 0.01, a tolerance parameter of 0.001, and while considering 5 spatial folds. Each model was initiated with 10 trees, and additional trees were incrementally added (in steps of 5) up to a maximum of 10,000, with the optimal number selected based on cross-validation tests. We evaluated the inferences using the area under the receiver operating characteristic (ROC) curve, also simply referred to as "area under the curve" (AUC). We further used the AUC metric to assess the capacity of our models trained on occurrence data < 2020 to predict > 2020 distribution of occurrence data. To assess how each environmental factor contributed to the different BRT models, we computed their relative influence (RI) in those models and their response curves showing how ecological suitability varies with one specific factor. RI values were obtained by evaluating the number of times a specific environmental factor was selected for splitting a tree, weighted by the squared improvement to the model as a result of each split, averaged over all trees (Elith et al., 2008).

We explored the four sets of environmental variables assembled by Dhingra and colleagues (Dhingra et al., 2016) and described above in the "Environmental data acquisition" subsection. The BRT analyses presented here were eventually performed based on set 2 for wild bird cases and set 4 for domestic bird cases. This selection is aligned with the methodology of Dhingra and colleagues (2016), prioritising variables which demonstrated the best predictive accuracy and clear epidemiological significance to minimise the potential for coincidental correlations. The RI values obtained when analysing each set of environmental variables separately are all reported in a table in Supplementary Information Resources S2.

Bird diversity indices calculation

Diversity index calculations were performed using the HPAI dataset. Cases lacking information on the date of collection, bird family, and subtype were excluded from the analyses. The diversity of HPAI cases across bird families was quantified using two indices: the Shannon diversity index and the Simpson diversity index. The Shannon index accounts for evenness of bird families (Shannon, 1948), whereas the Simpson index provides a measure of dominance (Simpson, 1949), emphasising the most abundant families in the dataset. Simpson index ranges between 0 and 1, where 1 represents infinite diversity and 0 no diversity. Calculations were done using two time points: before

526 and after 2020, and for various data classifications: overall and annually, across all bird families and specifically sea
527 bird families, as well as for all subtypes (HxNx) and those identified as H5N1 subtype, wild birds, and poultry. These
528 indices were calculated using the R package "vegan" (Oksanen et al., 2023): the dataset was first aggregated by year,
529 HPAI subtype and bird family, and we then used the "diversity" function to compute the Shannon and Simpson
530 indices for each year.
531

532 **Data and code accessibility**

533 R scripts and related files needed to run the analyses, as well as Supplementary Information Resources S1
534 (description and source of each environmental variable included in the original sets of variables) and S2 (mean
535 relative influence computed for the environmental variables within each considered set of variables), are all available
536 at https://github.com/sdellicour/h5nx_risk_mapping.
537

538 **Acknowledgments and funding**

539 MFVG and SD acknowledge funding from the European Union Horizon 2020 project MOOD (grant agreement
540 n°874850). MCD was supported by the UKRI GCRF One Health Poultry Hub (Grant No. B/S011269/1), one of twelve
541 interdisciplinary research hubs funded under the UK government's Global Challenge Research Fund Interdisciplinary
542 Research Hub initiative. MCD and SD are supported by the BELSPO project BE-PIN. SD also acknowledges support
543 from the *Fonds National de la Recherche Scientifique* (F.R.S.-FNRS, Belgium; grant n°F.4515.22), from the Research
544 Foundation - Flanders (*Fonds voor Wetenschappelijk Onderzoek - Vlaanderen*, FWO, Belgium; grant n°G098321N),
545 from the European Union Horizon 2020 project LEAPS (grant agreement n°101094685), from the ImmunReach
546 project funded by the *Institut d'Encouragement de la Recherche Scientifique et de l'Innovation de Bruxelles* (Innoviris,
547 Belgium), and from the doctoral network VIVACE funded by the Marie Skłodowska-Curie Actions (MSCA) of the
548 European Commission (grant agreement n°101167768).
549

550 **References**

551 Amirgazin A, Shevtsov A, Karibayev T, Berdikulov M, Kozhakhmetova T, Syzdykova L, Ramankulov Y, Shustov AV.
552 2022. Highly pathogenic avian influenza virus of the A/H5N8 subtype, clade 2.3.4.4b, caused outbreaks in
553 Kazakhstan in 2020. *PeerJ* **10**:e13038. doi:10.7717/peerj.13038

Bahl J, Pham TT, Hill NJ, Hussein ITM, Ma EJ, Easterday BC, Halpin RA, Stockwell TB, Wentworth DE, Kayali G, Krauss S, Schultz-Cherry S, Webster RG, Webby RJ, Swartz MD, Smith GJD, Runstadler JA. 2016. Ecosystem Interactions Underlie the Spread of Avian Influenza A Viruses with Pandemic Potential. *PLOS Pathogens* **12**:e1005620. doi:10.1371/journal.ppat.1005620

Banyard A, Begeman L, Black J, Breed A, Dewar M, Fijn R. 2023. Continued expansion of high pathogenicity avian influenza H5 in wildlife in South America and incursions in to the Antarctic Region. *OFFLU statement*.

Boulinier T. 2023. Avian influenza spread and seabird movements between colonies. *Trends in Ecology & Evolution* **38**:391–395. doi:10.1016/j.tree.2023.02.002

Bregnballe T, Herrmann C, Globig A, Günther A, Staubach C, Heise JN, Harder T, Beer M, Knief U, Heinicke T, Leivits M, Lundström K, Nurmoja I, Liang Y, Larsen LE, Hjulsager CK, Pohlmann A, Fox AD. 2024. Outbreaks of highly pathogenic avian influenza (HPAI) epidemics in Baltic Great Cormorant *Phalacrocorax carbo* colonies in 2021 and 2022. *Bird Study* 1–14. doi:10.1080/00063657.2024.2399168

Caliendo V, Lewis NS, Pohlmann A, Baillie SR, Banyard AC, Beer M, Brown IH, Fouchier RAM, Hansen RDE, Lameris TK, Lang AS, Laurendeau S, Lung O, Robertson G, Van Der Jeugd H, Alkie TN, Thorup K, Van Toor ML, Waldenström J, Yason C, Kuiken T, Berhane Y. 2022. Transatlantic spread of highly pathogenic avian influenza H5N1 by wild birds from Europe to North America in 2021. *Sci Rep* **12**:11729. doi:10.1038/s41598-022-13447-z

Campagna C, Uhart M, Falabella V, Campagna J, Zavattieri V, Vanstreels RET, Lewis MN. 2024. Catastrophic mortality of southern elephant seals caused by H5N1 avian influenza. *Marine Mammal Science* **40**:322–325. doi:10.1111/mms.13101

Center For International Earth Science Information Network-CIESIN-Columbia University. 2017. Gridded Population of the World, Version 4 (GPWv4): Population Density, Revision 11. doi:10.7927/H49C6VHW

Dezfuli A, Horton KG, Zuckerberg B, Schubert SD, Bosilovich MG. 2022. Continental Patterns of Bird Migration Linked to Climate Variability. *Bulletin of the American Meteorological Society* **103**:E536–E547. doi:10.1175/BAMS-D-21-0220.1

Dhingra MS, Artois J, Dellicour S, Lemey P, Dauphin G, Von Dobschuetz S, Van Boeckel TP, Castellan DM, Morzaria S, Gilbert M. 2018. Geographical and Historical Patterns in the Emergences of Novel Highly Pathogenic Avian Influenza (HPAI) H5 and H7 Viruses in Poultry. *Frontiers in Veterinary Science* **5**.

Dhingra MS, Artois J, Robinson TP, Linard C, Chaiban C, Xenarios I, Engler R, Liechti R, Kuznetsov D, Xiao X, Dobschuetz SV, Claes F, Newman SH, Dauphin G, Gilbert M. 2016. Global mapping of highly pathogenic avian influenza H5N1 and H5Nx clade 2.3.4.4 viruses with spatial cross-validation. *eLife* **5**:e19571. doi:10.7554/eLife.19571

Dusek RJ, Hallgrimsson GT, Ip HS, Jónsson JE, Sreevatsan S, Nashold SW, TeSlaa JL, Enomoto S, Halpin RA, Lin X, Fedorova N, Stockwell TB, Dugan VG, Wentworth DE, Hall JS. 2014. North Atlantic Migratory Bird Flyways Provide Routes for Intercontinental Movement of Avian Influenza Viruses. *PLOS ONE* **9**:e92075. doi:10.1371/journal.pone.0092075

ECDC. 2021. Avian influenza overview September – December 2021. https://www.ecdc.europa.eu/en/publications-data/avian-influenza-overview-september-december-2021

EFSA, Abrahantes JC, Aznar I, Catalin I, Kohnle L, Mulligan KF, Mur L, Stoicescu A, van Houtum A, Zancanaro G. 2025. Avian influenza annual report 2023. *EFS2* **23**. doi:10.2903/j.efsa.2025.9197

EFSA, Brouwer A, Gonzales J, Huneau A, Mulatti P, Kuiken T, Staubach C, Stegeman A, Antoniou S, Baldinelli F,

Van der Stede Y, Aznar I. 2019. Annual Report on surveillance for avian influenza in poultry and wild birds in Member States of the European Union in 2018. *EFS2* **17**. doi:10.2903/j.efsa.2019.5945

Elith J, H. Graham C, P. Anderson R, Dudík M, Ferrier S, Guisan A, J. Hijmans R, Huettmann F, R. Leathwick J, Lehmann A. 2006. Novel methods improve prediction of species' distributions from occurrence data. *Ecography* **29**:129–151.

Elsmo EJ, Wünschmann A, Beckmen KB, Broughton-Neiswanger LE, Buckles EL, Ellis J, Fitzgerald SD, Gerlach R, Hawkins S, Ip HS, Lankton JS, Lemley EM, Lenoch JB, Killian ML, Lantz K, Long L, Maes R, Mainenti M, Melotti J, Moriarty ME, Nakagun S, Ruden RM, Shearn-Bochsler V, Thompson D, Torchetti MK, Van Wettere AJ, Wise AG, Lim AL. 2023. Highly Pathogenic Avian Influenza A(H5N1) Virus Clade 2.3.4.4b Infections in Wild Terrestrial Mammals, United States, 2022. *Emerg Infect Dis* **29**:2451–2460. doi:10.3201/eid2912.230464

European Environment Agency (EEA). 2022. Landscape fragmentation pressure in Europe. https://www.eea.europa.eu/en/analysis/indicators/landscape-fragmentation-pressure-in-europe

FAO. 2023. Global consultation on highly pathogenic avian influenza (HPAI). FAO. doi:10.4060/cc7302en

FAO. 2005. Potential risk of Highly Pathogenic Avian Influenza (HPAI) spreading through wild water bird migration. https://openknowledge.fao.org/items/d6185856-dae8-4e8a-a345-1eb34e591a36

FAO, WHO and WOAH. 2023. Ongoing avian influenza outbreaks in animals pose risk to humans. *AnimalHealth*. https://www.fao.org/animal-health/news-events/news/detail/ongoing-avian-influenza-outbreaks-in-animals-pose-risk-to-humans/en

Forcey GM, Linz GM, Thogmartin WE, Bleier WJ. 2007. Influence of land use and climate on wetland breeding birds in the Prairie Pothole region of Canada. *Can J Zool* **85**:421–436. doi:10.1139/Z07-005

Gamarra-Toledo V, Plaza PI, Gutiérrez R, Inga-Diaz G, Saravia-Guevara P, Pereyra-Meza O, Coronado-Flores E, Calderón-Cerrón A, Quiroz-Jiménez G, Martinez P, Huamán-Mendoza D, Nieto-Navarrete JC, Ventura S, Lambertucci SA. 2023. Mass Mortality of Marine Mammals Associated to Highly Pathogenic Influenza Virus (H5N1) in South America. doi:10.1101/2023.02.08.527769

Giacinti JA, Signore AV, Jones MEB, Bourque L, Lair S, Jardine C, Stevens B, Bollinger T, Goldsmith D, British Columbia Wildlife AIV Surveillance Program (BC WASP), Pybus M, Stasiak I, Davis R, Pople N, Nituch L, Brook RW, Ojkic D, Massé A, Dimitri-Masson G, Parsons GJ, Baker M, Yason C, Harms J, Jutha N, Neely J, Berhane Y, Lung O, French SK, Myers L, Provencher JF, Avery-Gomm S, Robertson GJ, Barychka T, Gurney KEB, Wight J, Rahman I, Hargan K, Lang AS, Montevecchi WA, Burt TV, Brown MGC, Pekarik C, Thompson T, McLaughlin A, Willie M, Wilson L, Flemming SA, Ross MV, Leafloor J, Baldwin F, Sharp C, Lewis H, Beaumont M, Hanson A, Ronconi RA, Reed E, Campbell M, Saunders M, Soos C. 2024. Avian influenza viruses in wild birds in Canada following incursions of highly pathogenic H5N1 virus from Eurasia in 2021–2022. *mBio* **15**:e03203-23. doi:10.1128/mbio.03203-23

Gierak A, Śmietanka K. 2021. The impact of selected risk factors on the occurrence of highly pathogenic avian influenza in commercial poultry flocks in Poland. *Journal of Veterinary Research* **65**:45–52. doi:10.2478/jvetres-2021-0013

Gilbert M, Cinardi G, Da Re D, Wint WGR, Wisser D, Robinson TP. 2022a. Global chickens distribution in 2015 (5 minutes of arc). doi:10.7910/DVN/SXHLF3

Gilbert M, Cinardi G, Da Re D, Wint WGR, Wisser D, Robinson TP. 2022b. Global ducks distribution in 2015 (5 minutes of arc). doi:10.7910/DVN/S9ONXV

636 Gilbert M, Nicolas G, Cinardi G, Van Boeckel TP, Vanwambeke SO, Wint G, Robinson TP. 2018. Global distribution
637 data for cattle, buffaloes, horses, sheep, goats, pigs, chickens and ducks in 2010. *Scientific data* **5**:1–11.

638 Gilbert M, Pfeiffer DU. 2012. Risk factor modelling of the spatio-temporal patterns of highly pathogenic avian
639 influenza (HPAIV) H5N1: A review. *Spatial and Spatio-temporal Epidemiology* **3**:173–183.
640 doi:10.1016/j.sste.2012.01.002

641 Gilbert M, Slingenbergh J, Xiao X. 2008. Climate change and avian influenza. *Rev Sci Tech* **27**:459–466.

642 Gilbert M, Xiao X, Robinson TP. 2017. Intensifying poultry production systems and the emergence of avian influenza
643 in China: a 'One Health/Ecohealth' epitome. *Archives of Public Health* **75**:48. doi:10.1186/s13690-017-0218-
644 4

645 Graziosi G, Lupini C, Catelli E, Carnaccini S. 2024. Highly Pathogenic Avian Influenza (HPAI) H5 Clade 2.3.4.4b
646 Virus Infection in Birds and Mammals. *Animals* **14**:1372. doi:10.3390/ani14091372

647 Hijmans RJ. 2012. Cross-validation of species distribution models: removing spatial sorting bias and calibration with a
648 null model. *Ecology* **93**:679–688.

649 Hijmans RJ, Phillips S, Leathwick J, Elith J, Hijmans MRJ. 2017. Package 'dismo.' *Circles* **9**:1–68.

650 Hitch AT, Leberg PL. 2007. Breeding Distributions of North American Bird Species Moving North as a Result of
651 Climate Change. *Conservation Biology* **21**:534–539. doi:10.1111/j.1523-1739.2006.00609.x

652 Huang P, Sun L, Li J, Wu Q, Rezaei N, Jiang S, Pan C. 2023. Potential cross-species transmission of highly
653 pathogenic avian influenza H5 subtype (HPAI H5) viruses to humans calls for the development of H5-
654 specific and universal influenza vaccines. *Cell Discov* **9**:1–13. doi:10.1038/s41421-023-00571-x

655 Huang Y, Wille M, Dobbin A, Walzthöni NM, Robertson GJ, Ojkic D, Whitney H, Lang AS. 2014. Genetic Structure of
656 Avian Influenza Viruses from Ducks of the Atlantic Flyway of North America. *PLOS ONE* **9**:e86999.
657 doi:10.1371/journal.pone.0086999

658 Klaassen M, Wille M. 2023. Wild birds' plight and role in the current bird flu panzootic. *bioRxiv* 2023–05.

659 Knief U, Bregnballe T, Alfarwi I, Ballmann MZ, Brenninkmeijer A, Bzoma S, Chabrolle A, Dimmlich J, Engel E, Fijn R,
660 Fischer K, Hälterlein B, Haupt M, Hennig V, Herrmann C, In 'T Veld R, Kirchhoff E, Kristersson M, Kühn S,
661 Larsson K, Larsson R, Lawton N, Leopold M, Lilipaly S, Lock L, Marty R, Matheve H, Meissner W, Morrison
662 P, Newton S, Olofsson P, Packmor F, Pedersen KT, Redfern C, Scarton F, Schenk F, Scher O, Serra L,
663 Sibille A, Smith J, Smith W, Sterup J, Stienen E, Strassner V, Valle RG, Van Bemmelen RSA, Veen J,
664 Vervaeke M, Weston E, Wojcieszek M, Courtens W. 2024. Highly pathogenic avian influenza causes mass
665 mortality in Sandwich Tern *Thalasseus sandvicensis* breeding colonies across north-western Europe. *Bird*
666 *Conservation International* **34**:e6. doi:10.1017/S0959270923000400

667 Leguia M, Garcia-Glaessner A, Muñoz-Saavedra B, Juarez D, Barrera P, Calvo-Mac C, Jara J, Silva W, Ploog K,
668 Amaro, Lady, Colchao-Claux P, Johnson CK, Uhart MM, Nelson MI, Lescano J. 2023. Highly pathogenic
669 avian influenza A (H5N1) in marine mammals and seabirds in Peru. *Nat Commun* **14**:5489.
670 doi:10.1038/s41467-023-41182-0

671 Martin V, Pfeiffer DU, Zhou X, Xiao X, Prosser DJ, Guo F, Gilbert M. 2011. Spatial Distribution and Risk Factors of
672 Highly Pathogenic Avian Influenza (HPAI) H5N1 in China. *PLoS Pathog* **7**:e1001308.
673 doi:10.1371/journal.ppat.1001308

674 Neumann G, Kawaoka Y. 2024. Highly pathogenic H5N1 avian influenza virus outbreak in cattle: the knowns and
675 unknowns. *Nat Rev Microbiol* **22**:525–526. doi:10.1038/s41579-024-01087-1

676 Peacock T, Moncla L, Dudas G, VanInsberghe D, Sukhova K, Lloyd-Smith JO, Worobey M, Lowen AC, Nelson MI.

2024. The global H5N1 influenza panzootic in mammals. *Nature* 1–2. doi:10.1038/s41586-024-08054-z

Plaza PI, Gamarra-Toledo V, Euguí JR, Lambertucci SA. 2024. Recent Changes in Patterns of Mammal Infection with Highly Pathogenic Avian Influenza A(H5N1) Virus Worldwide. *Emerg Infect Dis* **30**. doi:10.3201/eid3003.231098

Prosser DJ, Teitelbaum CS, Yin S, Hill NJ, Xiao X. 2023. Climate change impacts on bird migration and highly pathogenic avian influenza. *Nat Microbiol* **8**:2223–2225. doi:10.1038/s41564-023-01538-0

Sacristán C, Ewbank AC, Ibáñez Porras P, Pérez-Ramírez E, De La Torre A, Briones V, Iglesias I. 2024. Novel Epidemiologic Features of High Pathogenicity Avian Influenza Virus A H5N1 2.3.3.4b Panzootic: A Review. *Transboundary and Emerging Diseases* **2024**:5322378. doi:10.1155/2024/5322378

Santos-Tovar A, Ramírez-Bastida P, Navarro-Sigüenza AG, Paz H, Ruiz-Rodríguez A, Vázquez-Reyes LD. 2024. Habitat fragmentation erodes taxonomic and functional diversity of waterbird communities of the South Pacific coast of Mexico. *Ornithol Res* **32**:124–134. doi:10.1007/s43388-024-00172-6

Scharlemann JP, Benz D, Hay SI, Purse BV, Tatem AJ, Wint GW, Rogers DJ. 2008. Global data for ecology and epidemiology: a novel algorithm for temporal Fourier processing MODIS data. *PloS one* **3**:e1408.

Sciensano. 2024. Avian Influenza: Numbers. *sciensano.be*. https://www.sciensano.be/en/health-topics/avian-influenza/numbers

Shannon CE. 1948. A Mathematical Theory of Communication. *Bell System Technical Journal* **27**:379–423. doi:10.1002/j.1538-7305.1948.tb01338.x

Simpson EH. 1949. Measurement of Diversity. *Nature* **163**:688–688. doi:10.1038/163688a0

Sultankulova KT, Argimbayeva TU, Aubakir NA, Bopi A, Omarova ZD, Melisbek AM, Karamendin K, Kydyrmanov A, Chervyakova OV, Kerimbayev AA, Burashev YD, Kasymbekov YT, Orynbayev MB. 2024. Reassortants of the Highly Pathogenic Influenza Virus A/H5N1 Causing Mass Swan Mortality in Kazakhstan from 2023 to 2024. *Animals* **14**:3211. doi:10.3390/ani14223211

Tuanmu M, Jetz W. 2014. A global 1-km consensus land-cover product for biodiversity and ecosystem modelling. *Global Ecology and Biogeography* **23**:1031–1045.

U.S. Department of Agriculture A and PHIS. 2024. HPAI Confirmed Cases in Livestock. https://www.aphis.usda.gov/livestock-poultry-disease/avian/avian-influenza/hpai-detections/hpai-confirmed-cases-livestock

Valavi R, Shafizadeh-Moghadam H, Matkan A, Shakiba A, Mirbagheri B, Kia SH. 2019. Modelling climate change effects on Zagros forests in Iran using individual and ensemble forecasting approaches. *Theor Appl Climatol* **137**:1015–1025. doi:10.1007/s00704-018-2625-z

Van Doren BM. 2022. How migratory birds might have tracked past climate change. *Proceedings of the National Academy of Sciences* **119**:e2121738119. doi:10.1073/pnas.2121738119

Vandegrift KJ, Sokolow SH, Daszak P, Kilpatrick AM. 2010. Ecology of avian influenza viruses in a changing world. *Annals of the New York Academy of Sciences* **1195**:113–128. doi:10.1111/j.1749-6632.2010.05451.x

Wille M, Atkinson R, Barr IG, Burgoyne C, Bond AL, Boyle D, Christie M, Dewar M, Douglas T, Fitzwater T, Hassell C, Jessop R, Klaassen H, Lavers JL, Leung KK -S., Ringma J, Sutherland DR, Klaassen M. 2024. Long-Distance Avian Migrants Fail to Bring 2.3.4.4b HPAI H5N1 Into Australia for a Second Year in a Row. *Influenza Resp Viruses* **18**:e13281. doi:10.1111/irv.13281

Wille M, Klaassen M. 2023. No evidence for HPAI H5N1 2.3.4.4b incursion into Australia in 2022. *Influenza Resp*

Viruses **17**:e13118. doi:10.1111/irv.13118

WOAH. 2024. Practical guide for authorised field responders to HPAI outbreaks in marine mammals. https://www.woah.org/app/uploads/2024/02/woah-practicalguide-forauthorisedfieldresponders-hpaimarinemammals-feb24.pdf

WOAH. 2023. Ongoing avian influenza outbreaks in animals pose risk to humans. https://www.who.int/news/item/12-07-2023-ongoing-avian-influenza-outbreaks-in-animals-pose-risk-to-humans

Worobey M, Gangavarapu K, E. Pekar J, B. Joy J, Moncla L, U. G. Kraemer M, Dudas G, Goldhill D, Ruis C, Malpica Serrano L, Ji X, G. Andersen K, O. Wertheim J, Lemey P, A Suchard M, L. Rasmussen A, Chand M, Groves N, G. Pybus O, P. Peacock T, Rambaut A, I. Nelson M. 2024a. Preliminary report on genomic epidemiology of the 2024 H5N1 influenza A virus outbreak in U.S. cattle (Part 1 of 2) - Influenza virus / H5N1-global. *Virological*. https://virological.org/t/preliminary-report-on-genomic-epidemiology-of-the-2024-h5n1-influenza-a-virus-outbreak-in-u-s-cattle-part-1-of-2/970

Worobey M, Gangavarapu K, E. Pekar J, B. Joy J, Moncla L, U. G. Kraemer M, Dudas G, Goldhill D, Ruis C, Malpica Serrano L, Ji X, G. Andersen K, O. Wertheim J, Lemey P, A Suchard M, L. Rasmussen A, Chand M, Groves N, G. Pybus O, P. Peacock T, Rambaut A, I. Nelson M. 2024b. Preliminary report on genomic epidemiology of the 2024 H5N1 influenza A virus outbreak in U.S. cattle (Part 2 of 2) - Influenza virus / H5N1-global. *Virological*. https://virological.org/t/preliminary-report-on-genomic-epidemiology-of-the-2024-h5n1-influenza-a-virus-outbreak-in-u-s-cattle-part-1-of-2/970

Yin S, Xu Y, Xu M, Jong MCM de, Huisman MRS, Contina A, Prins HHT, Huang ZYX, Boer WF de. 2022. Habitat loss exacerbates pathogen spread: An Agent-based model of avian influenza infection in migratory waterfowl. *PLOS Computational Biology* **18**:e1009577. doi:10.1371/journal.pcbi.1009577

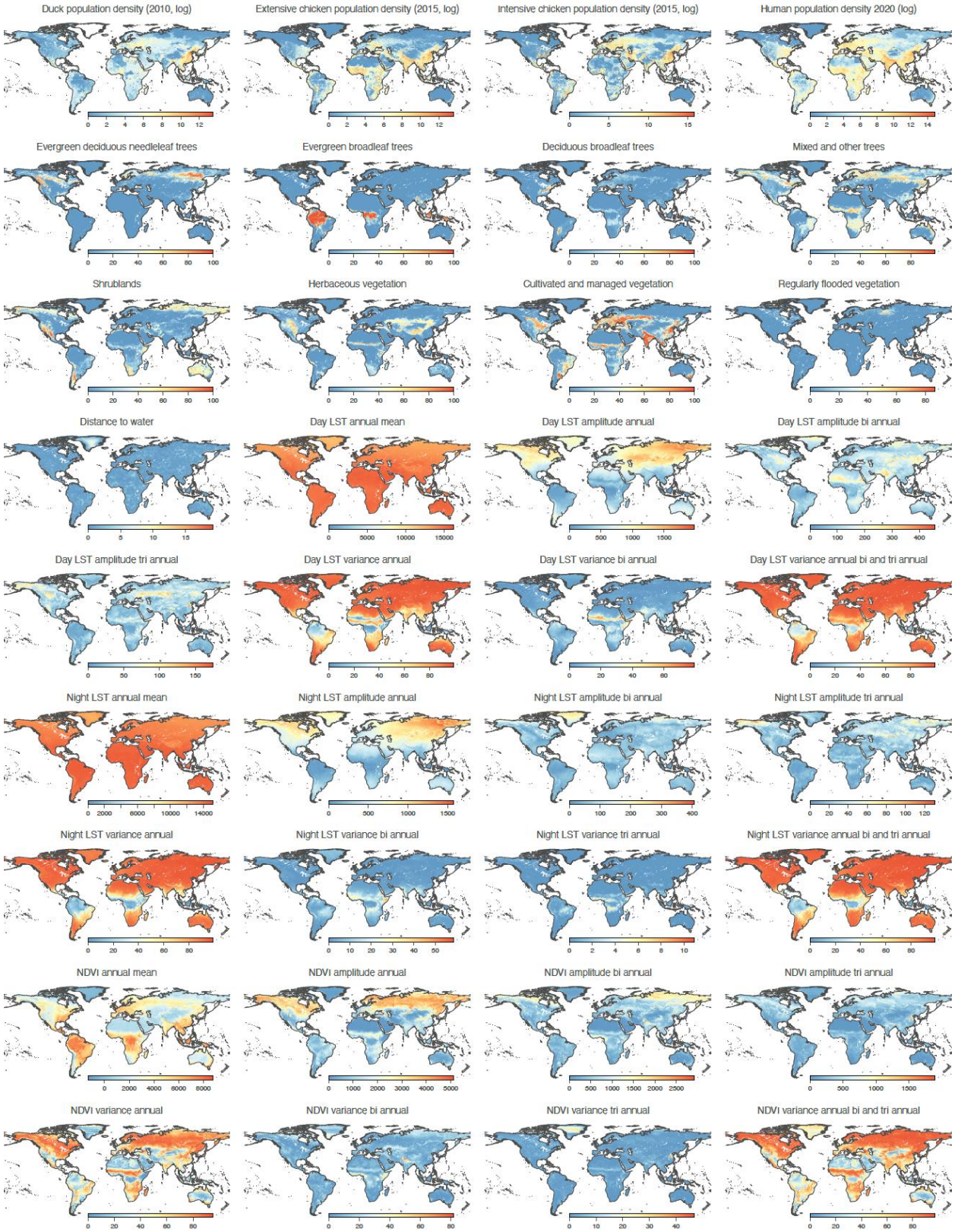

Figure S1 (part 1): environmental factors included in the ecological niche modelling. "LST" refers to "land surface temperature", "NDVI" to the "normalised difference vegetation index", and "EVI" to the "enhanced vegetation index".

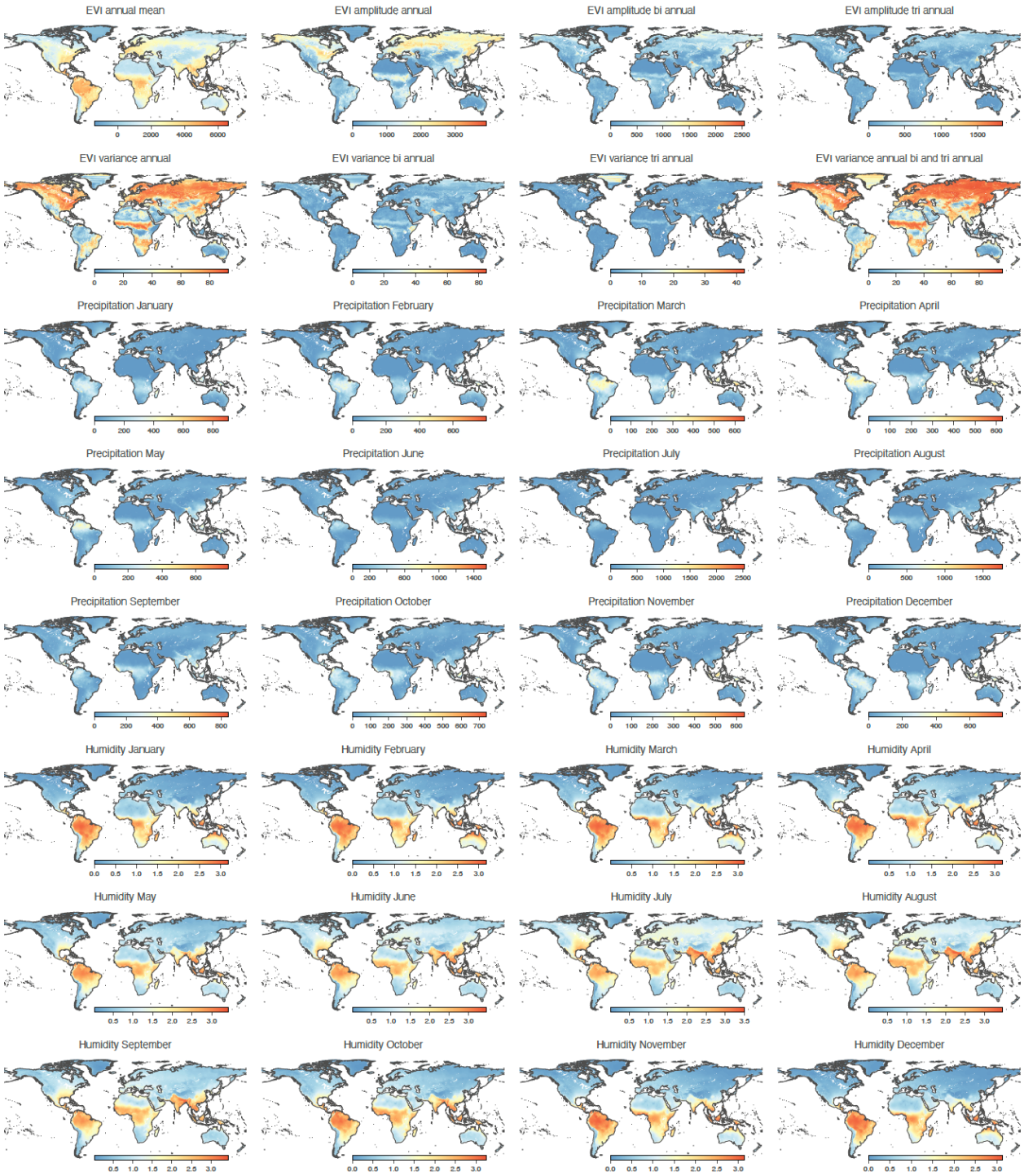

Figure S1 (part 2): environmental factors included in the ecological niche modelling. "LST" refers to "land surface temperature", "NDVI" to the "normalised difference vegetation index", and "EVI" to the "enhanced vegetation index".

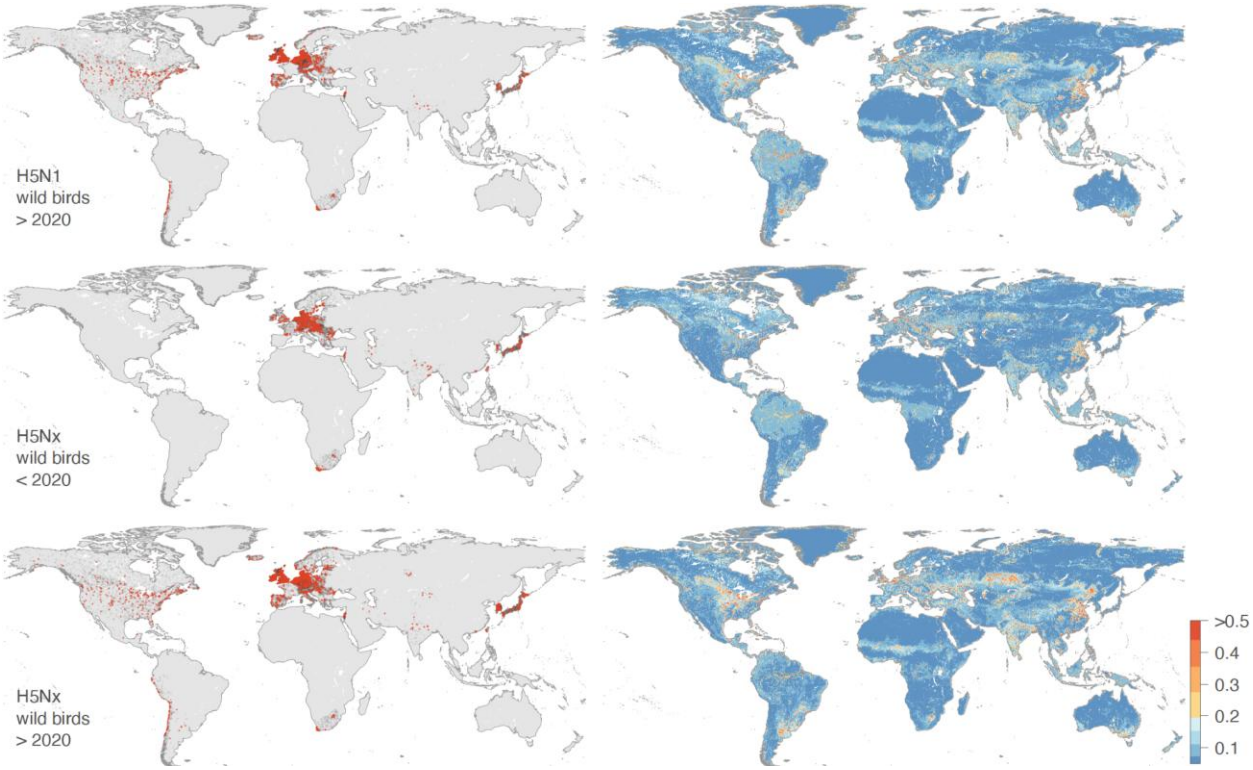

Figure S2 (part 1): comparison between the presence/pseudo-absence data used to train the ecological niche models (1° column) and the resulting ecological niche suitability maps (2° column). In the first column, presence and sampled pseudo-absence points are displayed as red and dark points, respectively. As detailed in the Materials and Methods section, pseudo-absence points were only sampled in countries in which there was at least one presence point (for either H5N1 or H5Nx, the considering time period, and bird populations). For Russia and China, we considered the admin-1 administrative areas instead of the country to define if pseudo-absence points should be sampled in the corresponding area. Specifically, for a given administrative region (i.e. a given country or admin-1 region in case of Russia or China) gathering at least one presence point, we sampled a number of pseudo-absence points equal to three times the number of presence points in that region. Furthermore, pseudo-absence points were sampled according to the log-transformed raster of human population density, which prevented the sampling of pseudo-absence in unpopulated areas non associated with any surveillance activity.

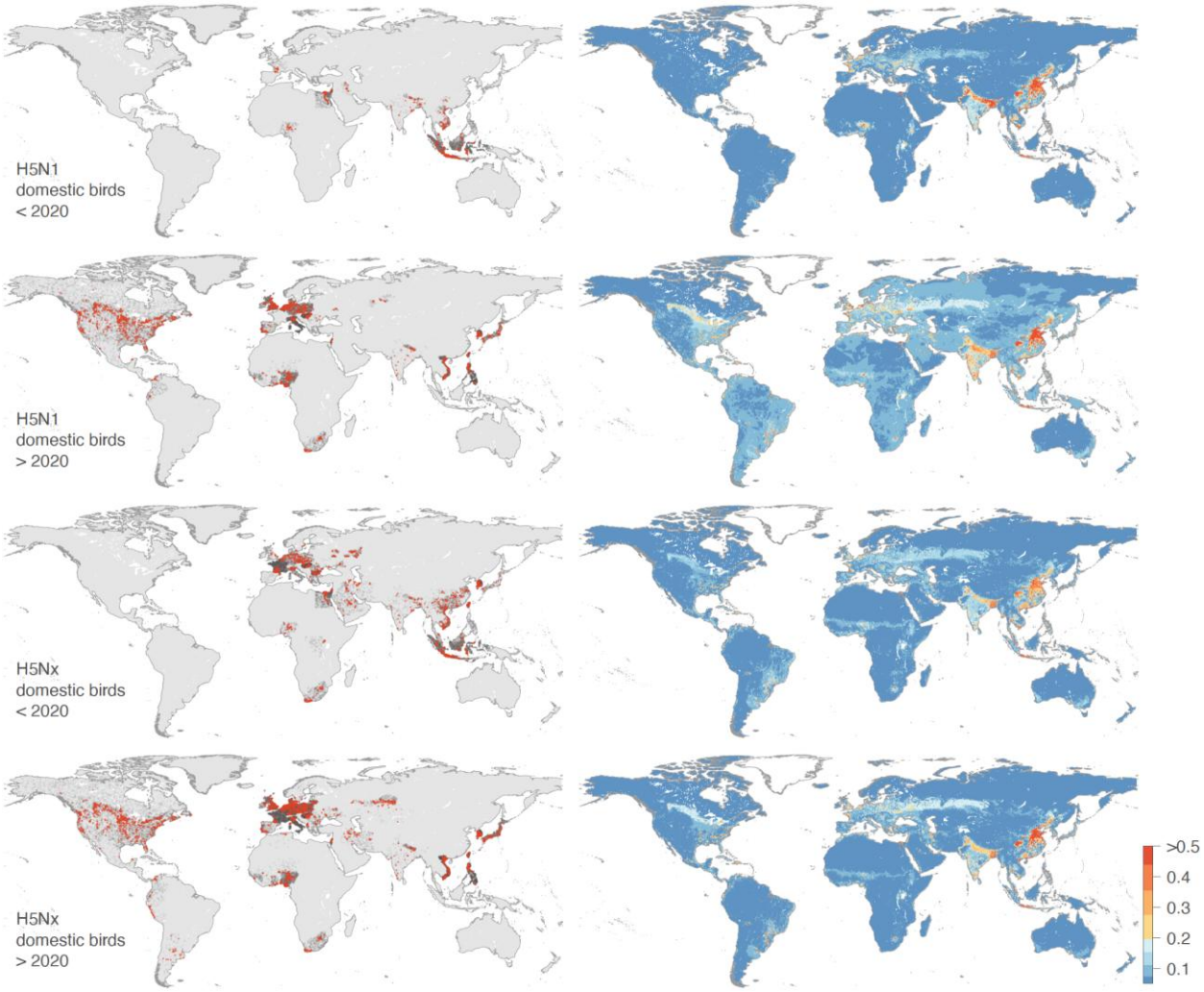

Figure S2 (part 2): comparison between the presence/pseudo-absence data used to train the ecological niche models (1° column) and the resulting ecological niche suitability maps (2° column). In the first column, presence and sampled pseudo-absence points are displayed as red and dark points, respectively. As detailed in the Materials and Methods section, pseudo-absence points were only sampled in countries in which there was at least one presence point (for either H5N1 or H5Nx, the considering time period, and bird populations). For Russia and China, we considered the admin-1 administrative areas instead of the country to define if pseudo-absence points should be sampled in the corresponding area. Specifically, for a given administrative region (i.e. a given country or admin-1 region in case of Russia or China) gathering at least one presence point, we sampled a number of pseudo-absence points equal to three times the number of presence points in that region. Furthermore, pseudo-absence points were sampled according to the log-transformed raster of human population density, which prevented the sampling of pseudo-absence in unpopulated areas non-associated with any surveillance activity.

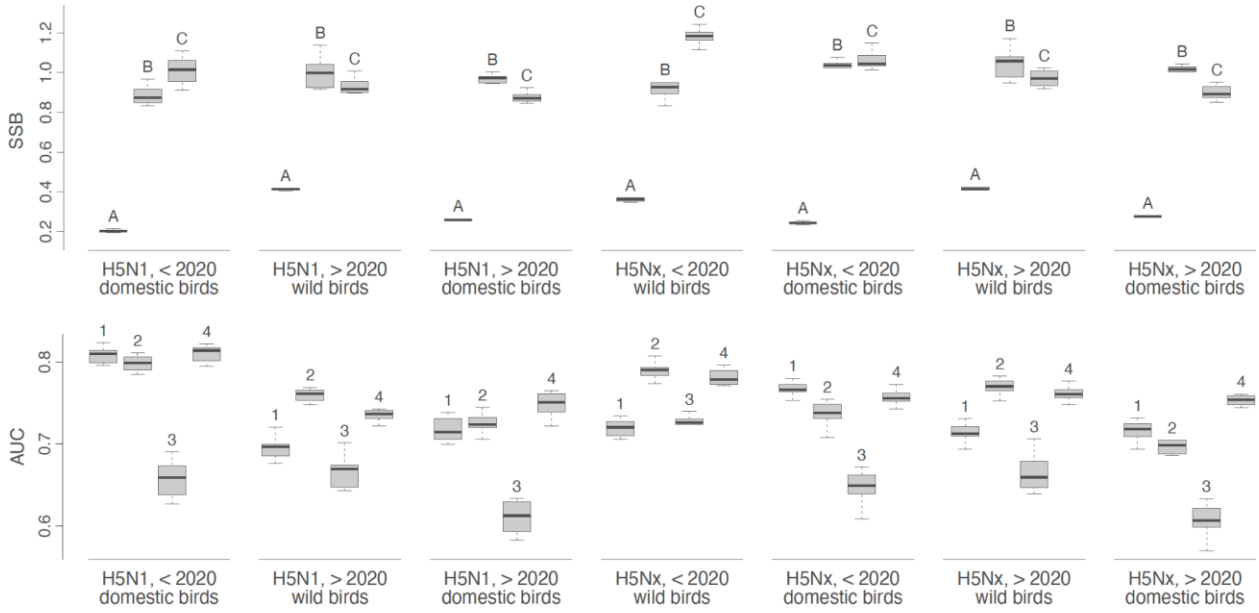

Figure S3: boxplots reporting the sorting sampling bias (SSB) and area under the curve (AUC) of the receiving operator curve metrics associated with various ecological niche models trained for H5N1 and H5Nx. For the SSB estimates, we report values obtained for the standard cross-validation (A), as well as spatial cross-validation procedures based on the reference points (B) and the blocks generation (C) approaches (see the Materials and Methods section for further detail). SSB estimates range from 0 to 1; values close to 0 indicate a strong impact of spatial autocorrelation on model training, while values close to 1 suggest little to no impact. The AUC metrics computed for the ecological niche models trained with the spatial cross-validation procedures based on the "epicentres", and we here report the values obtained for the models trained on each of the four distinct sets of environmental factors.

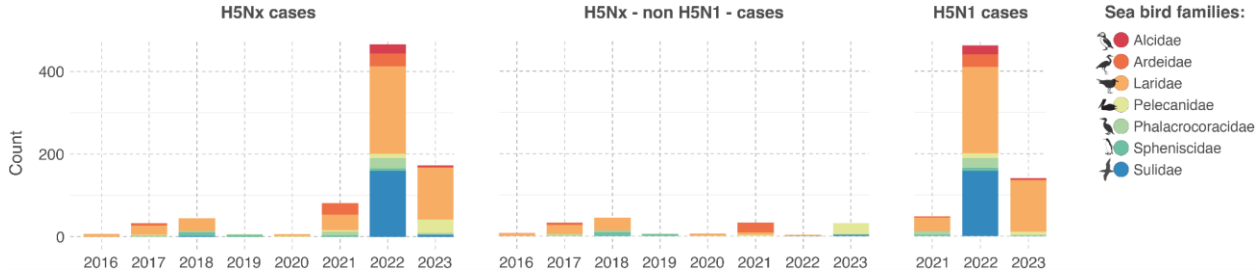

Figure S4: distribution of H5Nx and H5N1 occurrence records in sea birds from 2015 to 2023, categorised by bird family. The three panels successively show the total occurrence records for all H5Nx subtypes, occurrence records for non-H5N1 H5Nx subtypes, and all H5N1 occurrence records.

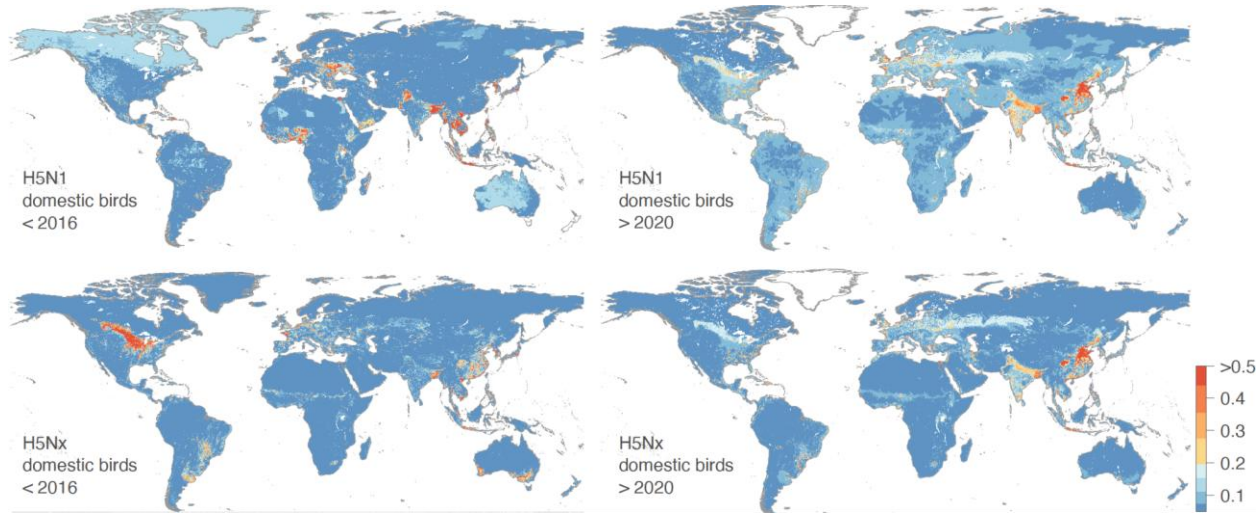

Figure S5: comparison between the ecological niche suitability estimated for H5N1 and H5Nx before 2016 and after 2020 for domestic bird populations. Specifically, we here compare the ecological niche models trained by Dhingra et al. (2016) on occurrence records collected between

January 2004 to March 2015 (< 2016) and the ecological niche models trained in the present study on occurrence records collected between January 2020 to March 2023 (> 2020).

Table S1: assessment of the predictive performance of ecological niche models to predict present and past ecological suitability maps. We here report, for each replicate analysis, a measure of the predictive performance of the trained ecological niche through the computation of the area under the receiver operating characteristic (ROC) curve, also simply referred to as "area under the curve" (AUC). (*) refers to AUC estimates obtained when assessing the capacity of models trained on occurrence data < 2020 to predict > 2020 distribution of occurrence data.

	Wild birds			Domestic birds					
	H5Nx			H5N1			H5Nx		
	< 2020	> 2020	>2020*	< 2020	> 2020	> 2020*	< 2020	> 2020	> 2020*
Replicate 1	0.899	0.793	0.700	0.832	0.812	0.769	0.833	0.791	0.755
Replicate 2	0.896	0.769	0.703	0.832	0.822	0.769	0.829	0.781	0.752
Replicate 3	0.895	0.796	0.707	0.834	0.820	0.770	0.818	0.784	0.743
Replicate 4	0.894	0.773	0.705	0.843	0.820	0.769	0.828	0.804	0.751
Replicate 5	0.893	0.797	0.706	0.837	0.816	0.770	0.828	0.780	0.752
Replicate 6	0.898	0.797	0.701	0.845	0.816	0.770	0.829	0.780	0.752
Replicate 7	0.897	0.798	0.700	0.835	0.816	0.769	0.827	0.775	0.750
Replicate 8	0.894	0.805	0.705	0.836	0.825	0.770	0.828	0.777	0.752
Replicate 9	0.894	0.770	0.702	0.834	0.813	0.769	0.828	0.779	0.750
Replicate 10	0.894	0.775	0.703	0.835	0.823	0.769	0.832	0.795	0.754

Table S2: relative influence (RI, in %) of each environmental variable in the respective ecological models trained on a specific dataset of occurrence data. A RI estimate was obtained for each replicate BRT analysis and we here report median as well as first and third quartile RI values.

	Wild birds			
	H5N1		H5Nx	
	< 2020	> 2020	< 2020	> 2020
Evergreen deciduous needleleaf trees	-	1.6 % [1.5-1.6]	1.6 % [1.3-1.7]	0.4 % [0.4-0.5]
Evergreen broadleaf trees	-	1.3 % [1.2-1.4]	0.1 % [0.1-0.1]	1.0 % [0.8-1.1]
Deciduous broadleaf trees	-	4.1 % [4.0-4.2]	1.6 % [1.5-1.8]	6.1 % [5.9-6.2]
Mixed and other trees	-	11.5 % [11.4-11.7]	5.3 % [4.9-5.4]	11.4 % [11.3-11.8]
Shrublands	-	2.3 % [2.0-2.3]	3.2 % [3.0-3.3]	2.4 % [2.1-2.7]
Herbaceous vegetation	-	8.8 % [8.8-9.0]	2.8 % [2.5-3.0]	9.5 % [9.5-9.6]
Cultivated and managed vegetation	-	4.4 % [4.3-4.5]	4.8 % [4.6-4.9]	5.8 % [5.4-6.1]
Regularly flooded vegetation	-	0.3 % [0.3-0.3]	0.1 % [0.1-0.1]	0.2 % [0.1-0.3]
Urban and built-up areas	-	39.3 % [39.0-39.9]	54.5 % [53.5-55.0]	37.5 % [36.5-38.2]
Open water areas	-	22.0 % [21.9-22.3]	25.5 % [25.3-25.8]	23 % [22.8-23.3]
Distance to water	-	4.1 % [3.9-4.3]	0.9 % [0.7-1.0]	2.8 % [2.4-3.1]
	Domestic birds			
	H5N1		**H5Nx**	
	< 2020	**> 2020**	**< 2020**	**> 2020**
Duck pop. density (2010, log)	18.2 % [17.8-18.4]	15.7 % [13.3-16.4]	28.7 % [28.4-28.8]	12.9 % [12.9-13.5]
Extensive chicken pop. density (2015, log)	4.4 % [4.2-4.5]	2.3 % [0.5-2.6]	3.9 % [3.7-4.0]	2.7 % [2.5-3.4]
Intensive chicken pop. density (2015, log)	8.5 % [8.4-8.7]	30.4 % [29.6-36.2]	29.6 % [29.3-30.1]	43.1 % [40.5-43.4]
Human pop. density (2020, log)	54.9 % [53.9-55.1]	20.7 % [20.4-21.6]	15.5 % [15.3-15.7]	14.9 % [14.8-15.2]
Cultivated and managed vegetation	9.5 % [9.3-9.7]	16.6 % [16.3-18.5]	7.1 % [7.0-7.2]	13.2 % [12.9-13.3]
Open water areas	0.5 % [0.5-0.6]	1.4 % [0.3-1.5]	0.0 % [0.0-0.0]	0.6 % [0.4-0.8]
Day LST annual mean	4.1 % [4.0-4.2]	12.9 % [9.6-13.3]	15.4 % [15.1-15.6]	13.0 % [12.4-13.9]